Magnetic ordering, electronic structure and magnetic anisotropy energy in the high-spin Mn_{10} single molecule magnet

Jens Kortus*
Max-Planck-Institut für Festkörperforschung, Heisenbergstr. 1, D-70569 Stuttgart, Germany

Tunna Baruah, N. Bernstein, and Mark R. Pederson
Center for Computational Materials Science, Naval Research Laboratory, Washington, DC 20375-5000, USA
(Dated: February 1, 2008)

We report the electronic structure and magnetic ordering of the single molecule magnet $[Mn_{10}O_4$(2,2'-biphenoxide)$_4Br_{12}]^{4-}$ based on first-principles all-electron density-functional calculations. We find that two of the ten core Mn atoms are coupled antiferromagnetically to the remaining eight, resulting in a ferrimagnetic ground state with total spin $S = 13$. The calculated magnetic anisotropy barrier is found to be 9 K in good agreement with experiment. The presence of the Br anions impact the electronic structure and therefore the magnetic properties of the 10 Mn atoms. However, the electric field due to the negative charges has no significant effect on the magnetic anisotropy.

The interest in magnetic molecular clusters of transition metal ions has been continuously growing since the observation of magnetic bi-stability of a purely molecular origin in the so-called Mn_{12}-ac,[1] which shows a magnetic hysteresis cycle below 4 K similar to that observed for bulk magnetic materials. The magnetic bi-stability associated with the hysteresis cycle has created an interest in these clusters for information storage, although at low temperature quantum effects affect the reversal of the magnetization, resulting in steps in the hysteresis.[2] This phenomenon of quantum tunneling of magnetization is governed by the magnetic anisotropy energy (MAE)[3] barrier which is due to directional dependencies of the spin-orbit-coupling operator.

Recently, Pederson and Khanna have developed a method for accounting for second-order anisotropy energies.[4] This method relies on an exact and simple expression for the spin-orbit coupling operator used in a second-order perturbative treatment to determine the dependence of the total energy on spin projection. Initial applications to the uniaxial Mn_{12}-ac lead to a density-functional-based second-order anisotropy energy[5] of 55.7 K, in agreement with the experimentally deduced values[6,7] of 54.8(3) K or 55.6 K.

Because the second-order anisotropy energy scales with the square of the magnetization it was generally believed that a high-spin ground state S would be beneficial for a large barrier. The $[Mn_{10}O_4$(2,2'-biphenoxide)$_4Br_{12}]^{4-}$ cluster has been reported to have a $S = 12$ high-spin ground state[8] but only a small energy barrier of about 7.7 K. In this work we investigate the electronic and magnetic properties and the magnetic anisotropy energy of this high-spin single molecule magnet. The information obtained here may be useful in the search for single molecule magnets with a greater magnetic anisotropy.

Fig. 1 shows the structure of the $[Mn_{10}O_4$(2,2'-biphenoxide)$_4Br_{12}]^{4-}$ molecular magnet. The 10 Mn atoms form a tetrahedron like structure with Mn atoms at the corners and at the middle of the tetrahedron edges. Two of the Mn atoms, the top and the bottom spheres in Fig. 1, are coupled antiferromagnetically to the rest of the Mn atoms. The Mn atoms are bridged by O atoms. The magnetic core is further stabilized by organic rings that are also connected to the O atoms. The negatively charged cluster is compensated by $[(CH_3CH_2)_3NH]_2[Mn(CH_3CN)_4(H_2O)_2]$ in the molecular crystal, but experimental results suggest that the magnetic anisotropy is due to the localized valences of the 10 Mn atoms.[8] In order to use the higher symmetry and make the problem computationally feasible, we carried out our calculation on the negatively charged $[Mn_{10}O_4$(2,2'-biphenoxide)$_4Br_{12}]^{4-}$ cluster which contains 114 atoms. The eight symmetry operations reduce the complete cluster to 18 inequivalent atoms.

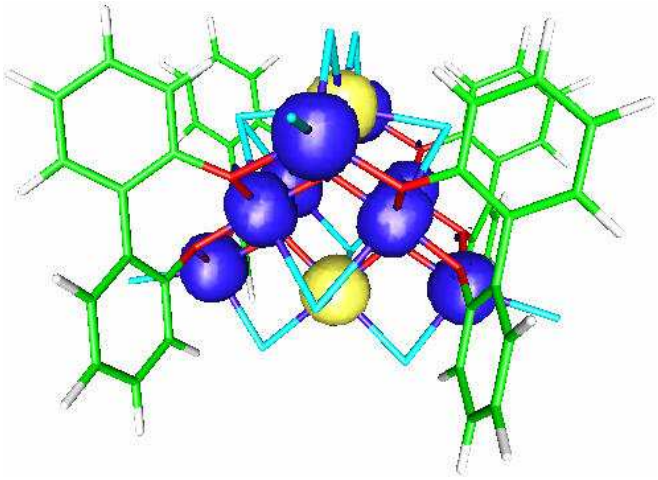

FIG. 1: The tetrahedron like structure of the ten Mn atoms and the surrounding organic rings. The Br atoms are not displayed for clarity. Density isosurfaces for $0.03\ e/a_B^3$ for majority (dark) and minority (light) spins on Mn atoms are shown. The plot clearly shows that the magnetic moment is localized at the Mn atoms, and it directly confirms the antiferromagnetic coupling of two of Mn atoms (large light spheres) to the remaining Mn atoms (large dark spheres).

The theoretical studies were carried out using a linear combination of atomic-orbitals molecular-orbital (LCAO-MO) approach within the density-functional framework.[9,10] The molecular orbitals were expanded as linear combinations of

TABLE I: The Gaussian basis set used for the calculation. The minimum and maximum exponent α of the bare Gaussians, the number of bare Gaussians, the number of contracted s-, p- and d-like basis functions.

	$\alpha_{\min}$	$\alpha_{\max}$	N_{bare}	s	p	d
Br	0.0781	7.9×10^6	21	11	6	4
Mn	0.0416	3.6×10^6	20	11	5	4
O	0.1049	6.1×10^4	13	8	4	3
C	0.0772	2.2×10^4	12	8	4	3
H	0.0745	77.84	6	5	3	1

Gaussian functions centered at the atomic sites. The calculations were carried out at the all-electron level and the multicenter integrals required in the solution of the Kohn-Sham equation were calculated by integrating numerically over a mesh of points.[11]

Our density functional-based calculations were performed with the all-electron Gaussian-orbital based Naval Research Laboratory Molecular Orbital Library (NRLMOL) program,[11,12,13,14,15,16] using the Perdew-Burke-Ernzerhof (PBE) generalized-gradient approximation for the exchange and correlation functional.[17] NRLMOL combines large Gaussian orbital basis sets, numerically precise variational integration and an analytic solution of Poisson's equation to accurately determine the self-consistent potentials, secular matrix, total energies and Hellmann-Feynman-Pulay forces. The exponents for the single Gaussian have been fully optimized for DFT calculations.[15] The basis set for the Mn_{10} cluster consisted of a total of 3756 contracted orbitals. The minimum and maximum exponent of the bare Gaussians, the number of bare Gaussians, and the number of contracted s-, p- and d-like basis functions are given in Table I for each atomic species. The contraction coefficients for atomic orbitals were obtained by performing an SCF-LDA calculation on the spherical unpolarized atom where the total energy of the atom was converged to within 10 meV. The basis functions that do not correspond to atomic wavefunction were constructed from the longest range bare Gaussians in the basis set.

Here we repeat some of the formulas needed for discussion of the magnetic anisotropy energy. The same definitions and notation are used as in Ref.4. In the absence of a magnetic field the second-order MAE Δ_2 resulting from the spin-orbit coupling, for an arbitrary symmetry, reduces to

$$\Delta_2 = \sum_{\sigma\sigma'} \sum_{ij} M_{ij}^{\sigma\sigma'} S_i^{\sigma\sigma'} S_j^{\sigma'\sigma}, \qquad (1)$$

which is a generalization of Eq. (19) of Ref.4. The matrix elements $S_i^{\sigma\sigma'} = \langle \chi^\sigma | S_i | \chi^{\sigma'} \rangle$ implicitly depend on two angles (θ, β) defining the axis of quantization. The matrix elements $M_{ij}^{\sigma\sigma'}$, which are related to of the induced orbital moment, are given by

$$M_{ij}^{\sigma\sigma'} = -\sum_{kl} \frac{\langle \phi_{l\sigma} | V_i | \phi_{k\sigma'} \rangle \langle \phi_{k\sigma'} | V_j | \phi_{l\sigma} \rangle}{\varepsilon_{l\sigma} - \varepsilon_{k\sigma'}}, \qquad (2)$$

where $\phi_{l\sigma}$, $\phi_{k\sigma}$ and $\varepsilon_{l\sigma}$ are, respectively, the occupied, unoccupied and the corresponding energies of states. V_i is same as defined in Eq. (7) of Ref.4 and is related to derivatives of the Coulomb potential. The matrix elements can be evaluated by integrating products of the Coulomb potential with partial derivatives of the basis functions. This procedure avoids the time consuming task of calculating the gradient of the Coulomb potential directly.

In addition to the magnetically interesting complex, the crystal also contains single Mn complexes to balance the charges. Using high-field EPR spectroscopy Barra *et al.*[8] found that this $[(CH_3CH_2)_3NH]_2[Mn(CH_3CN)_4(H_2O)_2]$ unit is paramagnetic. We also find that this unit is paramagnetic, with the Mn atom in a $+2$ charge state and a spin of S=5/2. The complex exhibits easy-plane behavior with an energy well of 0.1 K. We therefore focus the remainder of our work on the Mn_{10} unit only.

Calculations on a S=12 high spin state revealed that this spin state would not be magnetically stable because the Fermi levels in the majority and minority spin channel would not be aligned. The Fermi level misalignment indicated further transport of electrons of the minority to the majority spin channel. As a result we obtained a S=13 high spin state as the magnetic ground state instead of the S=12 state obtained from high-field EPR spectroscopy. Our result is consistent with experiment since it is difficult to differentiate experimentally between the two possibilities.[18]

A plot of the spin density shown in Fig. 1 clearly confirms the antiferromagnetic coupling of two of the Mn atoms to the remaining Mn atoms. The spin density around the minority spin Mn and the four majority spin Mn at the corners of the tetrahedron-like magnetic core show a nearly spherical spin density which one would expect for a closed d^5 shell. The other four Mn atoms which are on the edges of the tetrahedron (large dark spheres) show a less spherical spin density, indicating another charge state for these atoms. In order to analyze the magnetic ordering we calculated the spin density in spheres around the atoms. This gives a measure of the localized moment at the atom, but will generally underestimate the exact value. Using spheres with a radius of 2.23 a_B around the Mn atoms we obtained for the three non-equivalent Mn atoms (majority spin tetrahedron edge, majority spin tetrahedron vertex, and minority spin tetrahedron edge) a local moment of 3.61, 4.33 and -4.33 μ_B, respectively. This result suggests an ionic picture that the first Mn has an Mn^{3+} ($S = 2$) state, whereas the other two are Mn^{2+} ($S = 5/2$). This picture is fully in accord with the spin density plot in Fig. 1. Due to the symmetry of the cluster, the two types of majority spin Mn atoms have a multiplicity of 4 whereas the minority spin Mn atom has a multiplicity of 2, resulting in the previously mentioned $S = 4 \times 2 + 4 \times 5/2 - 2 \times 5/2 = 13$ magnetic ground state.

The electronic density of states (DOS) for the majority and minority spin channels is shown in Fig. 2. For each spin, the DOS is further decomposed into the $3d$ contributions of all Mn atoms. It is evident from the plot that the states around the Fermi level are clearly connected with $3d$ states of the Mn atoms. This result also agrees well with the experimental picture that the states near the Fermi level are well localized and do not show strong hybridization with other atoms, although

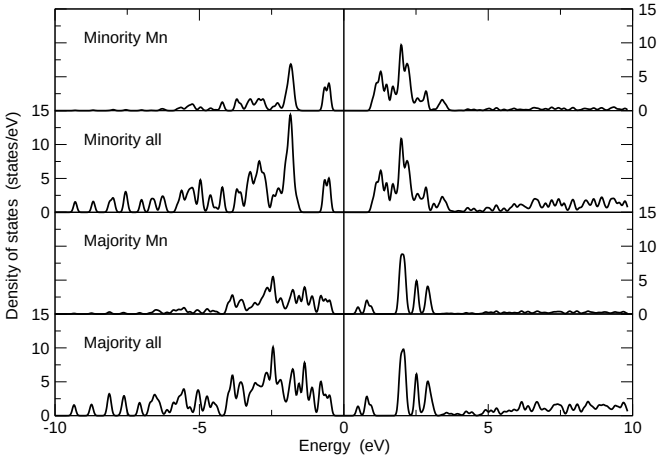

FIG. 2: Electronic density of states (DOS) broadened by 0.54 eV of Mn_{10} in the spin $S = 13$ configuration. For each spin the total DOS and the projected DOS of all Mn($3d$) are presented. The vertical line indicates the Fermi level.

we find some oxygen, bromine and nitrogen contributions for the occupied states.

Starting from the experimental geometry[18] we carried out about 30 steps of a conjugate-gradient algorithm using the Hellmann-Feynman-Pulay forces for optimization of the geometry. For each new geometry we calculated the complete Hamiltonian of the magnetic anisotropy and the second-order contribution to magnetic anisotropy barrier DS_z^2. In accord with experimental data, we find that the Mn_{10} single molecule magnet is an easy-axis system. The barrier showed no strong dependence on geometry varying between 8.8 K and 10.4 K with a value of 9.5 K for the lowest energy geometry. Expressing the barrier in the form of a simple spin Hamiltonian $H = DS_z^2$ we obtained a value of $D = -0.056$ K. For the calculation of the spin orbit matrix elements, we included all valence electrons and all unoccupied states in an energy window of 13.6 eV above the highest occupied state. The difference between the second-order treatment and exact diagonalization of the Hamiltonian including the spin-orbit matrix elements, which includes some higher order effects too, was of the order of 0.1 K.

Eq. 2 shows that the barrier is related to matrix elements between occupied and unoccupied orbitals in the majority and minority spin channels. In order to give a deeper insight into which states are forming the barrier, we analyze these contributions in more detail. First, we focus on the contributions of the different spin channels. Table II summarizes the result in form of the D parameter allowing only a given spin channel, for example including only matrix elements $M_{ij}^{\sigma\sigma'}$ between occupied majority states and unoccupied minority states, in the calculation of the barrier. All matrix elements from the occupied majority electrons prefer an easy-axis system, whereas the matrix elements from the occupied minority spin channel would result in an easy-plane system. Only due to the larger values of the contributions of the occupied majority spin channel the system ends up as an easy-axis system. This destructive interference between the different spin channels seems to be the reason for the small barrier compared with Mn_{12}. In Mn_{12} constructive interference between the different spin channels was observed.

occupied	unoccupied	D (K)	DS_z^2 (K)
majority	majority	-0.039	-6.6
majority	minority	-0.106	-17.9
minority	majority	0.034	5.7
minority	minority	0.055	9.3

TABLE II: The contributions of the different spin channels (see Eq. 2) to the magnetic anisotropy parameter D and the magnetic anisotropy energy DS_z^2.

Besides the spin channel contribution, we can analyze which electronic states contribute most to the matrix elements $M_{ij}^{\sigma\sigma'}$. In Fig. 3 we display plots of the square of the wavefunctions of the occupied majority state and the unoccupied minority state which contribute to the matrix element $M_{ij}^{\sigma\sigma'}$ with the largest absolute value. The view is from the top with respect to Fig. 1. It is clearly visible that the states of interest are d-states localized at the same Mn atom. In this case, the states are localized at the minority spin Mn atoms (light spheres in Fig. 1). In order to emphasize the d character of the wavefunctions, we have chosen the top view, although the wavefunctions of the other minority Mn atom are just below the top ones and are not visible.

While Mn is the only magnetically active species in the complex, the remaining atoms affect the magnetic properties of the molecule. In particular the electric field of the twelve Br^- ions can affect the MAE through its effects on the electronic structure and on the spin-orbit coupling. Effects of the Br ions on the electronic structure are of a chemical nature, and a detailed analysis is beyond the scope of this work. However, direct effects on the spin-orbit coupling energy could raise the possibility that even small variations in the positions of these ions could affect the magnetic properties of the molecule.

To measure the effects of the Br^- ions on the electronic structure we redid the calculations with various subsets of the Br^- ions. For each removed Br we also removed an extra electron, keeping the remaining molecule isoelectronic with the original complex. For these systems with either zero, four, or eight Br atoms, we observed a range of behaviors. In some cases the electronic structure near the Fermi level was similar to the original molecule, although it never showed truly rigid-band-like behavior. In other cases, however, the electronic structure changed significantly, sometimes completely closing the HOMO-LUMO gap. Associated with these electronic structure changes were large changes in the MAE, including changes in the magnitude of the anisotropy barrier, as well as instances of changes to an easy-plane system.

To measure the direct effect of the electric field of the Br ions on the spin-orbit coupling, external Coulomb potentials which acted to cancel the long range affects of the Br anions were added and the spin-orbit interaction and magnetic anisotropy were recomputed. This neutralized the electric

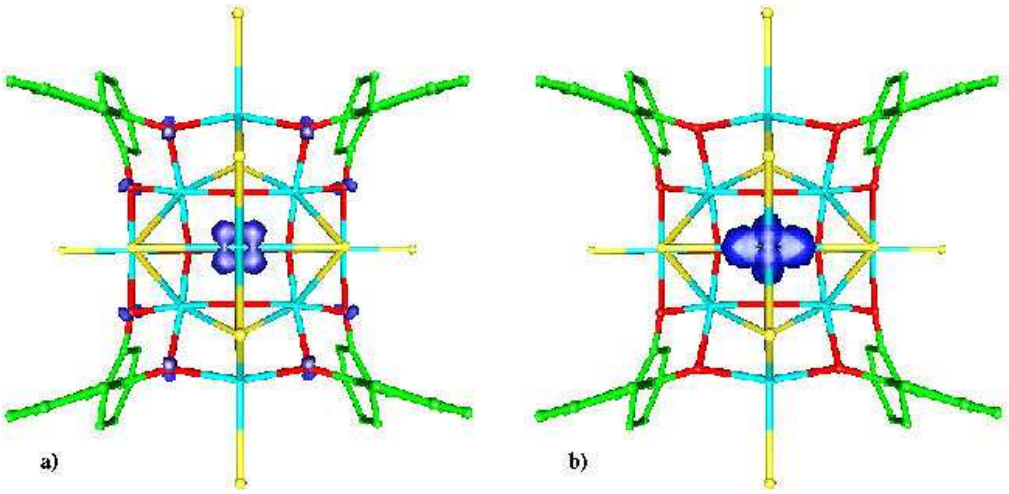

FIG. 3: Isolines at 0.005 e/a_B^3 of the square of the wavefunctions (occupied majority state (a) and unoccupied minority state (b)) which contribute most to the matrix elements $M_{ij}^{\sigma\sigma'}$. The view is from top with respect to the earlier figures. It is clearly visible that the matrix element connects majority and minority d-states at the same Mn atom.

field due to the Br^- ions near the Mn sites without changing the electronic structure of the molecule. We tested the effects with neutralizing charge distributions of various widths, and by neutralizing four, eight, or all twelve Br anions. The MAE changed by less than 1 K in all of these calculations. We therefore conclude that the electric fields created by the Br^- ions do not have a significant effect on the magnetic properties of the molecule.

In conclusion, we present a study of the electronic and magnetic properties of the Mn_{10} single molecule magnet. We confirm the experimentally suggested magnetic ordering, although we find that a state with $S = 13$ is the magnetic ground state in contrast to the $S = 12$ state suggested from high field EPR measurements.[8] In agreement with experiment we find the Mn_{10} unit is an easy-axis system with a small barrier of 9.5 K and the compensating cluster in the molecular crystal, which has one Mn atom with $S = 5/2$, is an easy plane system with a MAE of 0.1 K, negligible compared with the Mn_{10} unit. We show that the magnetic anisotropy is determined by a competition between different spin channels involved. The electric field caused by the negative charges of Br anions has no significant direct effect on the spin-orbit coupling or the MAE, although their chemical interactions do have significant effect on the electronic structure and therefore on the MAE. The states most important for the magnetic anisotropy energy involve transitions between occupied majority and unoccupied minority d-states at the same Mn-atom.

J.K. would like to thank the Schloeßmann Foundation for financial support and R. Sessoli for helpful discussions. The work was partially supported by the Office of Naval Research and the DOD HPCMO.

* Electronic address: j.kortus@fkf.mpg.de

[1] R. Sessoli, D. Gatteschi, A. Caneschi, and M. A. Novak, Nature (London) **365**, 141 (1993).

[2] J. Friedman, M. P. Sarachik, J. Tejeda, J. Maciejewski and R. Ziolo, Phys. Rev. Lett. **76**, 3820 (1996); L. Thomas, F. Lionti, R. Ballou, D. Gatteschi, R. Sessoli and B. Barbara, Nature (London) **383**, 145 (1996).

[3] J. Van Vleck, Phys. Rev. **52**, 1178 (1937).

[4] M. R. Pederson and S. N. Khanna, Phys. Rev. B **60**, 9566 (1999).

[5] M. R. Pederson and S. N. Khanna, Chem. Phys. Lett. **307**, 253, (1999); M. R. Pederson and S. N. Khanna, Phys. Rev. B **59**, R693 (1999).

[6] K. M. Mertes, Y. Suzuki, M. P. Sarachik, Y. Paltiel, H. Shtrikman, E. Zeldov, E. Rumberger, D. N. Hendrickson, and G. Christou, Phys. Rev. Lett. **87**, 227205 (2001).

[7] A. L. Barra, D. Gatteschi, and R. Sessoli, Phys. Rev. B **56**, 8192 (1997).

[8] A. L. Barra, A. Caneschi, D. Gatteschi, D. P. Goldberg, and R. Sessoli, J. Solid State Chemistry **145**, 484 (1999).

[9] P. Hohenberg and W. Kohn, Phys. Rev. **136**, B864 (1964).

[10] W. Kohn and L.J. Sham, Phys. Rev. **140**, A1133 (1965).

[11] M. R. Pederson and K. A. Jackson, Phys. Rev. B **41**, 7453 (1990).

[12] K. A. Jackson and M. R. Pederson, Phys. Rev. B **42**, 3276 (1990).

[13] A. Briley, M. R. Pederson, K. A. Jackson, D. C. Patton, and D.V. Porezag, Phys. Rev. A **58**, 1786 (1998).

[14] D. V. Porezag and M. R. Pederson, Phys. Rev. B **54**, 7830 (1996).

[15] D. V. Porezag and M. R. Pederson, Phys. Rev. A **60**, 9566 (1999).

[16] M. R. Pederson, D. V. Porezag, J. Kortus, and D. C. Patton, Phys. Stat. Sol. (b) **217**, 197 (2000).

[17] J. P. Perdew, K. Burke and M. Ernzerhof, Phys. Rev. Lett. **77**, 3865 (1996).

[18] R. Sessoli, private communication.